13th International Conference on Applications of Statistics and Probability in Civil Engineering, ICASP13
Seoul, South Korea, May 26-30, 2019

State-Space Models for Network-Scale Analysis of Bridge Inspection Data

Zachary Hamida
Ph.D. Candidate, Dept. of Civil, Geologic and Mining Engineering, Polytechnique Montreal, Montreal, CANADA

James-A. Goulet
Professor, Dept. of Civil, Geologic and Mining Engineering, Polytechnique Montreal, Montreal, CANADA

ABSTRACT: Visual inspection is one of the main techniques for monitoring the deterioration in networks of bridges. Visual inspection data commonly display inconsistencies due to the subjective nature of the evaluation and because different individuals perform the inspections over time. One of the main challenges when interpreting visual inspections is differentiating between measurement errors and legitimate changes in a structure's condition. This study proposes a state-space model for modeling the deterioration behaviour while accommodating the inspector-induced uncertainty. The proposed framework allows modeling inspections uncertainty according to the current structure's state as well as the variability associated with each inspector. The predictive capacity of the proposed framework is verified with synthetic inspection data, where the true deterioration state is known.

1. INTRODUCTION

Visual inspections are considered by many infrastructures owners as the default option for a network-scale monitoring [6, 7, 11]. This type of inspection has the advantage of providing direct information about the structure health. These information are based on a broad structural evaluation which does not target a specific type of damage or a structural component [1].

Although visual inspections is a popular monitoring approach, along with many advantages, the monitoring system suffers from shortages that limit its efficiency. Visual inspections are performed by different individuals over time, therefore, it is common to have inconsistencies in the recorded data. These inconsistencies introduce difficulties in differentiating between measurement errors and legitimate changes in a structure's condition. Moreover, the frequency of visual inspections performed varies among bridges, typically ranging from one year to over four years.

The uncertainty and insufficiency of monitoring data for each bridge cause difficulties in developing accurate structural degradation models. This study aims at developing a machine learning framework well suited for the network-scale analysis of transportation infrastructure. The core objective is to forecast the degradation of different structural elements over time, along with quantifying the speed and acceleration of this degradation. State-space models are employed to model the structural degradation of bridges based on visual inspection data. The proposed state-space model formulation incorporates an uncertainty modeling framework tailored for the visual inspection data. This framework allows modeling inspections uncertainty based on a current structure's condition and the inspector's variability.

1.1. Context & Notations

The data of a visual inspections system can be categorized into three levels: the *network level*, the

bridge level and the *element level*. The *network level* defines the transportation network regional properties (i.e. inspection code, country, ..., etc.). Following the *network level*, is the *bridge level* defined by the set of bridges $\mathcal{B} = \{b_1, b_2, \ldots, b_{\mathtt{B}}\}$. This level describes the characteristics of each bridge b_j included in the transportation network (i.e. geolocations, traffic loads, ..., etc.). The last level is the *element level* defined by the set of structural elements $\mathcal{E} = \{e_1^j, e_2^j, \ldots, e_{\mathtt{E_j}}^j\} \in b_j \subset \mathcal{B}$. This level defines the characteristics of the structural elements within each bridge (i.e. material, type, ..., etc.). The deterioration information collected through inspections are added to the hierarchy at the *element level*. These information include the inspection time t, the engineer I_i from the group of inspectors $\mathcal{I} = \{I_1, I_2, \ldots, I_{\mathtt{I}}\}$ responsible for evaluating the bridges in $\mathcal{B}$ and the condition of the structural element $\tilde{y} \in [l, u]$, with l representing the worst possible condition and u representing a perfect condition. The $\sim$ in $\tilde{y}$ is utilized to differentiate between observations in the bounded space $[l, u]$ and unbounded space $[-\infty, \infty]$ which is further detailed in section 2.2.2.

2. METHODOLOGY

This section describes the proposed framework for modeling the deterioration behaviour and quantifying visual inspections uncertainty.

2.1. State-Space Model

State-space models are well suited for *time-series* data and allow estimating the *hidden states* of the system from imperfect observations. The *hidden states* here refer to the unobservable states of the system. A *State-space model* is composed of two models: an *observation model* and a *transition model*. The formulas describing each model are,

$$\overbrace{\boldsymbol{y}_t = \boldsymbol{C}\boldsymbol{x}_t + \boldsymbol{v}_t}^{\text{observation model}}, \overbrace{\boldsymbol{v}_t : \boldsymbol{V} \sim \mathcal{N}(\boldsymbol{v}; \boldsymbol{0}, \boldsymbol{R}_t)}^{\text{observation errors}} \quad (1)$$

$$\underbrace{\boldsymbol{x}_t = \boldsymbol{A}\boldsymbol{x}_{t-1} + \boldsymbol{w}_t}_{\text{transition model}}, \underbrace{\boldsymbol{w}_t : \boldsymbol{W} \sim \mathcal{N}(\boldsymbol{w}; \boldsymbol{0}, \boldsymbol{Q}_t)}_{\text{process errors}}, \quad (2)$$

where $\boldsymbol{y}_t$ represents the observations, $\boldsymbol{C}$ is the observation matrix, $\boldsymbol{x}_t$ is the state vector at time t: $\boldsymbol{x}_t : \boldsymbol{X} \sim \mathcal{N}(\boldsymbol{x}, \boldsymbol{\mu}_t, \boldsymbol{\Sigma}_t)$, $\boldsymbol{A}$ is the state transition matrix, $\boldsymbol{v}_t$, $\boldsymbol{w}_t$ are the observation and process errors and $\boldsymbol{R}_t, \boldsymbol{Q}_t$ represent the observations and transition covariance matrices respectively. Different *state-space models* algorithms exist in the literature for different types of problems [3, 4, 5]. In this study, the estimation for the hidden states is done through the *Kalman Filter* (KF) [5] expressed in the short form as follows,

$$\begin{aligned}(\boldsymbol{\mu}_{t|t}, \boldsymbol{\Sigma}_{t|t}, \mathcal{L}_t) = \text{Kalman Filter}(&\boldsymbol{\mu}_{t-1|t-1}, \\ &\boldsymbol{\Sigma}_{t-1|t-1}, \boldsymbol{y}_t, \boldsymbol{A}_t, \boldsymbol{Q}_t, \boldsymbol{C}_t, \boldsymbol{R}_t),\end{aligned} \quad (3)$$

whereby $\mathcal{L}_t$ represent the log-likelihood for observation y_t and $\boldsymbol{\mu}_{t|t}$, $\boldsymbol{\Sigma}_{t|t}$ refer to the posterior expected value and the posterior covariance at time t respectively, given observations $\boldsymbol{y}_{1:t}$. In addition to KF, *Kalman Smoother* (KS) [8] is also utilized to refine the filtered estimates of KF.

2.2. Quantifying Visual Inspections Uncertainty

This section presents the proposed framework for quantifying the uncertainty of visual inspections.

2.2.1. Inspector-Induced Uncertainty

Visual inspections are performed by different inspectors $I_i \in \mathcal{I} = \{I_1, I_2, \ldots, I_{\mathtt{I}}\}$ over time, therefore, it is common to observe variability in the recorded data [9]. This variability is mainly attributed to the subjective nature of the evaluation. The variability in the observations is commonly quantified in *state-space models* through estimating a single *standard deviation* parameter σ_V common for all observations so that $v_{t,k}^j : V \sim \mathcal{N}(v; 0, \sigma_V^2)$. However, because each inspector may have a different variability, the *state-space model* is formulated to account for the inspector-dependent uncertainty. Each inspector I_i is assigned a *standard deviation* parameter $\sigma_V(I_i)$ to be estimated from the data. This allows characterizing inconsistencies that may exist in a sequence of observations obtained from different inspectors.

2.2.2. State-Dependant Uncertainty

In addition to estimating the uncertainty $\sigma_V(I_i)$ for each inspector, it is required to take into account that inspection uncertainty also depends on the element's condition. For example, if the structural element $e_k^j \in b_j$ is in a perfect condition ($\tilde{x}_k^j = u$), with

$\tilde{x}_k^j$ representing the true condition of e_k^j, then an inspector I_i is less likely to misjudge its condition. Hence, a small uncertainty should be associated with the observation $\tilde{y}_k^j$ for structural element with a perfect condition. Similarly for structural elements with a poor condition ($\tilde{x}_k^j = l$). On the other hand, for structural elements with a partial damage (e.g. $\tilde{x}_k^j = \frac{l+u}{2}$), the prospect of misjudging the structural element condition becomes higher. Thus, a higher uncertainty should be associated with the observation $\tilde{y}_k^j$ in such cases. The aforementioned uncertainty characteristics can be accommodated within the *time-series* analysis by applying a non-linear *transformation* on the state space. This *transformation* is done through a *transformation function* that maps each point from the original space to a point in the transformed space $g : \tilde{\mathbb{X}} \to \mathbb{X}$. Applying a proper *transformation function* in this context allows the observation and transition uncertainty to become a function of the structural element's state $\tilde{x}$. In addition, a byproduct of *space transformation* is that it constraints the state $\tilde{x}$ within the feasible interval of the state $[l,u]$. To attain both of the aforementioned properties, a step function with special characteristics is proposed. These characteristics are: linear middle span with $1:1$ slope ratio and non-linear ends with definite and known first derivative.

The proposed *transformation function* that is found to fulfill the desired characteristics is described by,

$$g(x) = \begin{cases} \frac{1}{\Gamma(\alpha)} \int_0^{x^{\frac{1}{\alpha}}} t^{\alpha-1} e^{-t} dt, & x > \frac{u+l}{2}, \\ x, & x = \frac{u+l}{2}, \\ -\frac{1}{\Gamma(\alpha)} \int_0^{x^{\frac{1}{\alpha}}} t^{\alpha-1} e^{-t} dt, & x < \frac{u+l}{2}. \end{cases} \quad (4)$$

This function $g(x)$ is a piecewise step function that maps $x \in [-\infty, \infty]$, labelled as the *transformed space*, to $\tilde{x} \in [l,u]$ labelled as the *original space*. The *transformation function* inverse $g^{-1}(\tilde{x})$ is given by,

$$g^{-1}(\tilde{x}) = \begin{cases} \left[\frac{1}{\Gamma(\alpha)} \int_0^{\tilde{x}} t^{\alpha-1} e^{-t} dt\right]^{\alpha}, & \frac{u+l}{2} < \tilde{x} \leq u \\ \tilde{x}, & \tilde{x} = \frac{u+l}{2} \\ -\left[\frac{1}{\Gamma(\alpha)} \int_0^{\tilde{x}} t^{\alpha-1} e^{-t} dt\right]^{\alpha}, & l \leq \tilde{x} < \frac{u+l}{2}. \end{cases} \quad (5)$$

The parameter α in both equations 5 & 4 is described by: $\alpha = 2^{-n}$. The role of the parameter n in the previous equation is to control the smoothness at the *transformation function* ends. For $n = 1$, the *transformation function* has smooth edges. As the parameter n value increases, the edges become sharper. However, for all n, the slope ratio remains fixed at $1:1$ for the middle span. This implies that the transformation is linear for all cases when the transformed value is near the centre of the feasible interval $[l,u]$. Moreover, it is noticed that for $n \geq 5$, the change in the shape of the *transformation function* is insignificant. Therefore, the possible values for the parameter n can be limited to $n = \{1,2,3,4,5,6\}$. Figure 1 presents examples of applying *space transformation* on the PDFs of two Normal distributions (Figure 1a) using Equation 4. In Figure 1a, the PDF with dashed-line illustrates how the probability content is adjusted when the expected value of the state in the *transformed space* is near the bounds $[l,u] = [25,100]$. On the other hand, when the expected value of the state is closer to the middle span (continuous-line PDF), the PDF in the *original space* (Figure 1b) reflects subtle differences from the PDF in the *transformed space*.

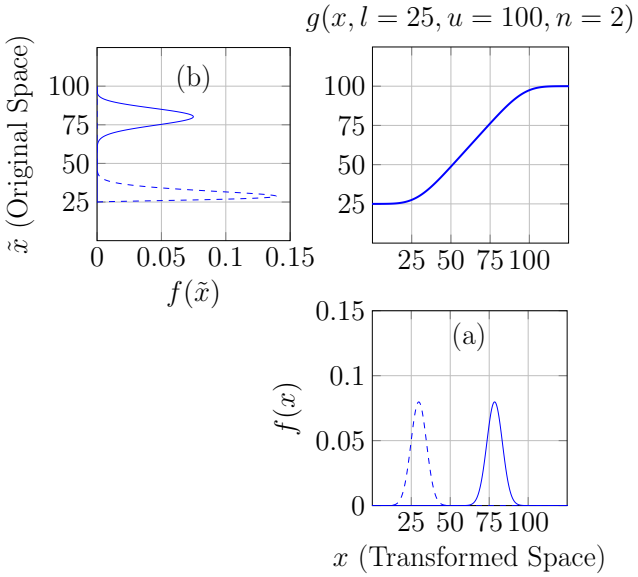

Figure 1: Examples of State Transformation with the Proposed Transformation Function.

Identifying the parameter n that best suit the problem context is done through the parameter estimation framework described in section 2.5.

2.3. Deterioration Model Constraints

The uncertainty and insufficiency of the inspection data for each bridge may result in unrealistic trends in the *time-series* data of the structural elements. For example, a set of observations may wrongfully indicate that an element's condition is improving over time without interventions being made on the structure. In order to prevent such a problem, constraints are applied for each time step. The constraint ensures that the expected value of the element condition between any consecutive time steps t and $t+1$ is not improving. This is achieved by constraining the expected value of the speed $\dot{\mu}$ along with the $2\sigma^{\dot{x}}$ confidence interval to be non-positive $\dot{\mu}+2\sigma^{\dot{x}} \leq 0$. The PDF Truncation method [10] is employed to handle this constraint in the *state-space model*.

2.4. Modeling Structural Degradation

The proposed framework for modeling the degradation process in structural elements is based on *state-space models*. The goal of this framework is to represent the degradation behaviour by a *kinematic model* that includes the element condition x, degradation speed $\dot{x}$ and acceleration $\ddot{x}$ as defined by,

$$\underbrace{\begin{bmatrix} x_t \\ \dot{x}_t \\ \ddot{x}_t \end{bmatrix}}_{\boldsymbol{x}_t} = \underbrace{\begin{bmatrix} 1 & \Delta t & \frac{\Delta t^2}{2} \\ 0 & 1 & \Delta t \\ 0 & 0 & 1 \end{bmatrix}}_{\boldsymbol{A}} \cdot \underbrace{\begin{bmatrix} x_{t-1} \\ \dot{x}_{t-1} \\ \ddot{x}_{t-1} \end{bmatrix}}_{\boldsymbol{x}_{t-1}} + \underbrace{\begin{bmatrix} w_t \\ \dot{w}_t \\ \ddot{w}_t \end{bmatrix}}_{\boldsymbol{w}_t}, \quad (6)$$

where $\boldsymbol{x}_t$ and $\boldsymbol{x}_{t-1}$ are the state vector at time t and $t-1$, $\boldsymbol{A}$ describes the model *kinematics* for transitioning from $\boldsymbol{x}_{t-1}$ to $\boldsymbol{x}_t$ and $\boldsymbol{w}_t$ is the model error vector. The *kinematic model* in Equation 6 is employed within the proposed framework to characterize the degradation behaviour in bridges $\mathcal{B}$. Therefore, for each structural element $e_k^j \in b_j$, the *transition model* that describes the deterioration process from time $(t-1)$ to time (t) is,

$$\boldsymbol{x}_{t,k}^j = \boldsymbol{A}\boldsymbol{x}_{t-1,k}^j + \boldsymbol{w}_t, \quad (7)$$

where $\boldsymbol{x}_{t,k}^j$ is the state vector at time t consisting of the condition $x_{t,k}^j$, the speed of degradation $\dot{x}_{t,k}^j$ and the acceleration $\ddot{x}_{t,k}^j$. The expected value of each component in the state vector $\boldsymbol{x}_{t,k}^j$ is represented by $\mu_{t,k}^j$ for the condition, $\dot{\mu}_{t,k}^j$ for the speed and $\ddot{\mu}_{t,k}^j$ for the acceleration. The matrix $\boldsymbol{A}$ in the *transition model* represents the *transition matrix* and $\boldsymbol{w}_t : \boldsymbol{W} \sim \mathcal{N}(\boldsymbol{w}; \boldsymbol{0}, \boldsymbol{Q}_t)$ represents the model error vector. The *observation model* for this *Kalman Filter* is described by,

$$y_{t,k}^j = \boldsymbol{C}\boldsymbol{x}_{t,k}^j + v_{t,k}^j, \quad (8)$$

where $y_{t,k}^j$ is the transformed state observation, $\boldsymbol{C}$ is the observation matrix, $\boldsymbol{x}_{t,k}^j$ is the system state and $v_{t,k}^j : V \sim \mathcal{N}(v; 0, \sigma_V^2(I_i))$ is the observation error with $\sigma_V(I_i)$ being the *standard deviation* of the error associated with the observations of inspector $I_i \in \mathcal{I}$. Figure 2 illustrates the details and the steps of the proposed degradation modeling framework.

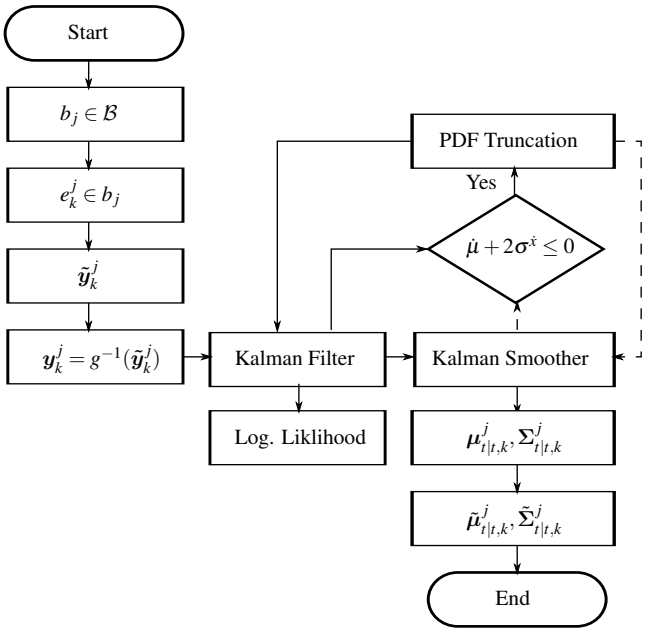

Figure 2: Framework of Structural Degradation Model

As shown in Figure 2, the framework starts with the observation $\tilde{y}_{t,k}^j \in [l,u]$ representing the condition of structural element $e_{t,k}^j \in b_j \subset \mathcal{B}$. The observation $\tilde{y}_{t,k}^j$ is passed in the *transformation function* presented in Equation 5 to obtain the transformed state observation $y_{t,k}^j \in [-\infty, \infty]$. Following the transformation step, the observations are ready for the *time-series* analysis through the *Kalman Filter* and *Kalman Smoother*. For any *time-series*

data $\boldsymbol{y}_k^j$, the *Kalman Filter* starts at time ($t = 0$) with an initial estimate for the state expected value vector $\boldsymbol{\mu}_{0,k}^j$ and the covariance matrix $\boldsymbol{\Sigma}_{0,k}^j = \text{diag}\left[{\sigma_{0,k}^x}^j, {\sigma_{0,k}^{\dot{x}}}^j, {\sigma_{0,k}^{\ddot{x}}}^j\right]^2$. The initial state is propagated in time by using the *prediction step* and the *update step* of the *Kalman Filter*. After each *update step* in the *Kalman Filter*, the constraint $\dot{\mu}_{t|t,k}^j + 2\sigma_{t|t,k}^{\dot{x},j} \leq 0$ is examined. This constraint ensures that the model estimate does not indicate that the structural element is improving over time. If the aforementioned constraint is violated, the PDF truncation method is employed to restrain the estimate of the speed $\dot{x}_{t|t,k}^j$ within the feasible bounds. Following the filtering step, the *Kalman Smoother* is utilized to refine the state estimates of KF and the initial estimate of the initial state at time $t = 0$. Because the number of observations $\boldsymbol{y}_k^j$ is limited per structural element, the refined estimate for the initial state $\boldsymbol{x}_{0,k}^j$ can be further improved in the parameter estimation framework described in the next section. After the smoothing step, the framework output $\boldsymbol{\mu}_{t|t,k}^j$, $\boldsymbol{\Sigma}_{t|t,k}^j$ is back-transformed to the original space $\tilde{\boldsymbol{\mu}}_{t|t,k}^j \in [25, 100]$, $\tilde{\boldsymbol{\Sigma}}_{t|t,k}^j$ for interpretation and analysis. This back-transformation step is done through the *transformation function* described in Equation 4. The following section describes the unknown model parameters and the estimation method.

2.5. Model Parameters & Estimation Framework

The unknown model parameters to be estimated from the inspection data are: the inspectors *standard deviations* $\sigma_V(I_i)$, the *standard deviation* of the *transition model* error σ_W, the *transformation function* parameter n and the initial estimate for the state $\{\dot{\mu}_0, \ddot{\mu}_0, \sigma_0^x, \sigma_0^{\dot{x}}, \sigma_0^{\ddot{x}}\}$ which will be common for all structural elements e_k^j. The parameters are grouped in the following set:

$$\mathcal{P} = \Big\{ \underbrace{\sigma_V(I_1), \sigma_V(I_2), \cdots, \sigma_V(I_{\mathtt{I}})}_{\text{Inspector std.}}, \overbrace{\sigma_W}^{\text{Process error std.}}, \underbrace{n}_{\text{Transform. Param.}}, \overbrace{\dot{\mu}_0, \ddot{\mu}_0, \sigma_0^x, \sigma_0^{\dot{x}}, \sigma_0^{\ddot{x}}}^{\text{Initial state.}} \Big\}. \tag{9}$$

The initial estimate for the expected condition $\mu_{0,k}^j$ is omitted from the set $\mathcal{P}$, because it is assumed equal to the first observation $\mu_{0,k}^j = y_{1,k}^j$ in each *time-series*. This assumption is reasonable because the deterioration analysis are rendered with a relatively small time step ($\Delta t = 1$ year) and the fact that the initial estimate of $\mu_{0,k}^j$ is later updated by the *Kalman Smoother*. The parameter estimation framework for the parameters $\mathcal{P}$ is based on the *Maximum Likelihood Estimate* (MLE) method. The MLE estimate is obtained through maximizing the joint prior probability of observations while assuming the observations to be independent. Thus, the likelihood for a sequence of observations can be obtained through the following product,

$$p(y_{1:\mathtt{T}}|\mathcal{P}) = \prod_{t=1}^{\mathtt{T}} p(y_t|y_{1:t-1}, \mathcal{P}). \tag{10}$$

In order to avoid numerical instabilities, the natural logarithm is taken for the likelihood estimate. Hence, Equation 10 becomes the *log-likelihood* estimate described by,

$$\ln p(y_{1:\mathtt{T}}|\mathcal{P}) = \sum_{t=1}^{\mathtt{T}} \ln p(y_t|y_{1:t-1}, \mathcal{P}). \tag{11}$$

Because the analysis in the proposed framework are performed on a network scale, the *log-likelihood* estimate is taken for the inspection sequences of all the structural elements $e_k^j \; \forall j,k$ combined. Therefore, the network-scale *log-likelihood* becomes,

$$\ln p(y_{1:\mathtt{T}_k,1:\mathtt{E}_j}^{1:\mathtt{B}}|\mathcal{P}) = \sum_{j=1}^{\mathtt{B}} \sum_{k=1}^{\mathtt{E}_j} \sum_{t=1}^{\mathtt{T}_k} \ln p(y_{t,k}^j|y_{1:t-1,k}^j, \mathcal{P}), \tag{12}$$

whereby $\mathtt{B}$ is the total number of bridges, $\mathtt{E}_j$ is the total number of structural elements and $\mathtt{T}_k$ is the total number of observations for the k-th structural element. The *log-likelihood* defined in Equation 12 represents the *log-likelihood* estimate for observations $y_{t,k}^j$ in the *transformed space*. Thus, the *log-likelihood* estimate is obtained from a Normal PDF. However, in the original space, the PDF of the state is not defined by a Normal distribution. This is due to the non-linearity in the *transformation function*. Because the *time-series* analysis are intended for

the observations in the original space, it is required to rely on the *log-likelihood* estimate $\mathcal{L}(\mathcal{P})$ from the PDF in the original space. This estimate can be obtained by multiplying the *log-likelihood* estimate by the derivative of the transformation function g as follows,

$$\mathcal{L}(\mathcal{P}) = \sum_{j=1}^{\mathtt{B}} \sum_{k=1}^{\mathtt{E}_j} \sum_{t=1}^{\mathtt{T}_k} \left(\ln p(y_{t,k}^j | y_{1:t-1,k}^j, \mathcal{P}) \times \left| \frac{\partial}{\partial x} g(x = y_{t,k}^j, n) \right|^{-1} \right). \tag{13}$$

The term $\frac{\partial}{\partial x} g(x,n)$ represent the first derivative of the proposed *transformation function* $g(x,n)$, which can be described analytically by,

$$\frac{\partial}{\partial x} g(x,n) = \frac{e^{-x^{\frac{1}{\alpha}}}}{\alpha \Gamma(\alpha)}, \ \alpha = 2^{-n}. \tag{14}$$

From Equation 13, in order to identify the set of parameters $\mathcal{P}^*$ that maximizes the *log-likelihood* estimate, the following optimization problem is to be solved,

$$\begin{aligned} \mathcal{P}^* = \arg\max_{\mathcal{P}} \quad & \mathcal{L}(\mathcal{P}), \\ \text{subject to:} \quad & \dot{\mu}_{t|t,k}^j \leq 0, \\ & 1 \leq n \leq 6, \ \forall n \in \mathbb{Z} \\ & \sigma_V(I_i) \geq 0, \ \forall I_i \in \mathcal{I}, \\ & \sigma_W \geq 0, \\ & \sigma_0^x, \sigma_0^{\dot{x}}, \sigma_0^{\ddot{x}} \geq 0. \end{aligned} \tag{15}$$

Solving this optimization problem is possible through the *Newton-Raphson* algorithm [2]. Note that other optimization algorithms remain to be tested in order to identify the optimization procedure that best suit the problem.

3. Deterioration Analyses

This section presents the analyses performed using the proposed framework on inspection data.

3.1. Data Description

The dataset utilized in this study is synthetic data that is analogous to real inspection dataset obtained from a network of bridges. The total number of structural elements e_k^j in the synthetic dataset is $\mathtt{E} = 19879$. The structural elements considered in this analysis are of an element type *beam*. The health condition of the structural elements is represented by a continuous numerical value within the range $[l,u] = [25,100]$. An evaluation of $\tilde{y} = 25$ refers to the worst possible condition for the structural element, while $\tilde{y} = 100$ indicates a perfect condition. The synthetic inspection data is generated through the *observation model* with a set of synthetic inspectors $\mathcal{I} = \{I_1, I_2, \ldots, I_{229}\}$ each having an error *standard deviation* $\sigma_V(I_i) \in [1,5]$.
Moreover, in the real dataset, the majority of structural elements has a *time-series* with 3 to 5 inspections $\boldsymbol{y}_k^j$, while very few structural elements have 6 or 8 inspections. Therefore, the number of observations $\boldsymbol{y}_k^j$ in each synthetic *time-series* is determined through weighted integer sampling, with the weights decided according to the real *time-series* dataset. This step is done to ensure that the synthetic data is analogous to the main characteristics in the real inspection data. The synthetic observations are generated in the *transformed space* based on a *transformation function* with parameter $n = 2$. The *standard deviation* of the model process error is assumed to be $\sigma_W = 10^{-2}$.

3.2. Model Verification & Analyses with Synthetic Inspection Data

The main goal of performing analysis with synthetic data is to verify the predictive capacity of the proposed deterioration model with a datasets that is analogous to the real dataset. In addition, it is possible to assess the estimation of the model parameters since the true parameters are available.
Estimating the model parameters based on the synthetic dataset is done by solving the optimization problem defined in Equation 15. Solving this optimization problem can be achieved iteratively through a *Newton-Raphson* gradient optimization framework. The set of model parameters $\mathcal{P}^*$ estimated from the synthetic inspection data is shown in Table 1 except for the parameters $\sigma_V(I_i)$ which are shown in Figure 3. From Figure 3, the initial value for all $\sigma_V(I_i)$, represented by the dashed line, is obtained from an initial *Newton-Raphson* optimization step that assumes a single σ_V for all

Table 1: Estimated Model Parameters from Synthetic Inspection Data.

σ_w	$\dot{\mu}_0$	$\ddot{\mu}_0$	σ_0^x	$\sigma_0^{\dot{x}}$	$\sigma_0^{\ddot{x}}$
9.434×10^{-4}	-1.652×10^{-4}	-1.078×10^{-4}	1.878	0.10005	0.07694

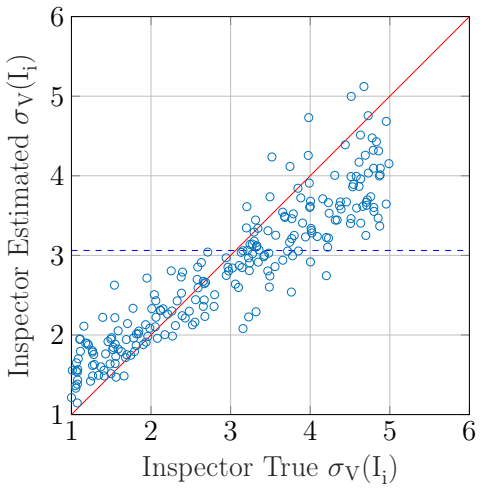

Figure 3: Scatter Plot of Inspectors True $\sigma_V(I_i)$ vs. Estimated $\sigma_V(I_i)$ (Transformed Space) with a Dashed Line Representing the Initial Value at the Start of the Optimization.

inspectors $I_i \in \mathcal{I}$. By considering the alignment among the true and estimated $\sigma_V(I_i)$, the scatter plot in Figure 3 confirms that the proposed method is capable of estimating the inspectors uncertainties from the network-scale deterioration data.

Following the assessment of the estimated model parameters $\mathcal{P}^*$, the overall performance of the deterioration model is examined with a test set of $\mathtt{E_t} = 3980$ structural elements e_k^j which amount to roughly 20% of the synthetic dataset size $\mathtt{E}$. The deterioration forecast is assessed for a period of 10 years for each structural element e_k^j. The yearly average of the forecast absolute error in the expected condition $\mu_{t|t,k}^j$, the expected speed $\dot{\mu}_{t|t,k}^j$ and the expected acceleration $\ddot{\mu}_{t|t,k}^j$ are shown in Figure 4. From Figure 4, it can be noticed that the yearly average of the absolute errors in each category increases monotonically over the forecast time. Moreover, the bias in the expected condition of the forecast is examined with scatter plots generated at different years. The graphs shown in Figure 5 illustrates the true condition $\tilde{x}_{t,k}^j$ versus the model expected condition $\tilde{\mu}_{t|t,k}^j$ generated at forecast years $\{1, 5, 10\}$. It is noticed from Figure 5 that the deterioration model maintain a good predictive capacity up to 5 years of forecast. Thereafter, the prediction error becomes significant as shown in the scatter plot at year 10.

4. Conclusion

In this study, a deterioration model for visual inspections of a network of bridges is proposed. This model enables quantifying the uncertainty of visual inspection data through estimating the uncertainty associated with each inspector as well as considering the inspection uncertainty dependent on the deterioration state. The analyses with synthetic data have demonstrated a promising performance for the model in estimating the uncertainty associated with the inspectors. Moreover, the deterioration analyses with the synthetic data have shown a good predictive capacity for the proposed deterioration model. Especially for the short term forecast up to 5 years where the estimated condition and the true condition have had a high correlation. However, analyses with the long term forecast have shown that further improvements are required in the framework. Therefore, further assessments to examine some of the model hypothesis, such as the model constraints, the initial speed estimate and/or the algorithm utilized in estimating the model parameter are to be examined in order to improve the model long-term performance.

Acknowledgements

This project is funded by Ministère des Transports, de la Mobilité durable et de l'Électrification des transports (MTMDET).

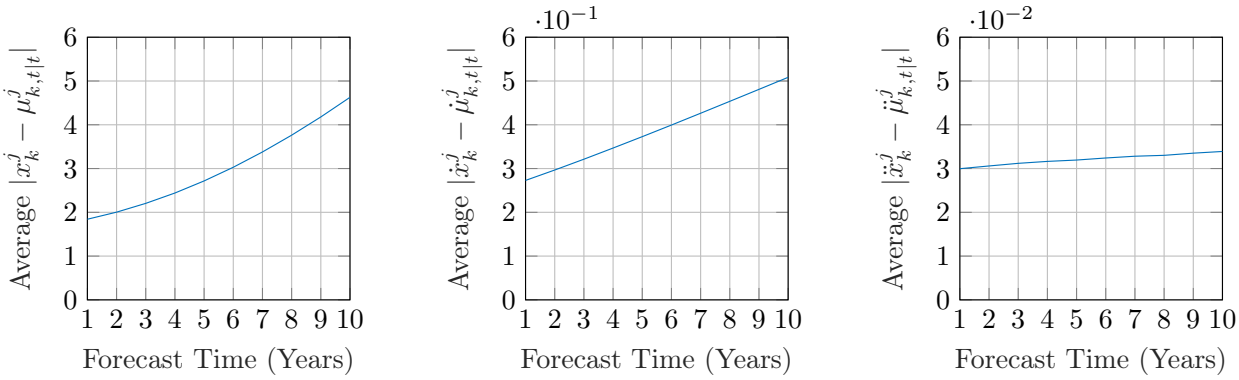

Figure 4: Average Error in Forecast Time for the Expected Condition, Speed and Acceleration.

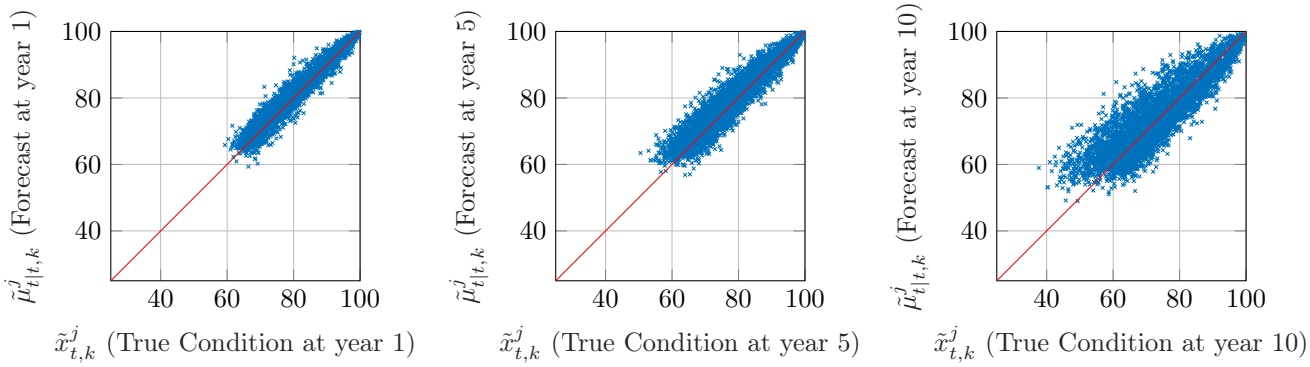

Figure 5: Scatter Plot for the Model Estimate of the Condition $\tilde{\mu}_{t|t,k}^j$ vs. the True Condition $\tilde{x}_{t,k}^j$ at Years 1, 5 and 10.

5. REFERENCES

[1] Agdas, D., Rice, J. A., Martinez, J. R., and Lasa, I. R. (2015). "Comparison of visual inspection and structural-health monitoring as bridge condition assessment methods." *Journal of Performance of Constructed Facilities*, 30(3), 04015049.

[2] Bonnans, J.-F., Gilbert, J. C., Lemaréchal, C., and Sagastizábal, C. A. (2013). *Numerical optimization: theoretical and practical aspects*. Springer Science Business Media.

[3] Del Moral, P. (1996). "Non-linear filtering: interacting particle resolution." *Markov processes and related fields*, 2(4), 555–581.

[4] Julier, S. J. and Uhlmann, J. K. (2004). "Unscented filtering and nonlinear estimation." *Proceedings of the IEEE*, 92(3), 401–422

[5] Kalman, R. E. (1960). "Contributions to the theory of optimal control." *Bol. Soc. Mat. Mexicana*, 5(2), 102–119.

[6] Ministère des Transports, de la Mobilité Durable et de l'Électrification des Transports (2014). *Manuel d'Inspection des Structures* (Jan).

[7] Moore, M., Phares, B. M., Graybeal, B., Rolander, D., and Washer, G. (2001). "Reliability of visual inspection for highway bridges, volume i." *Report no.*

[8] Rauch, H. E., Striebel, C., and Tung, F. (1965). "Maximum likelihood estimates of linear dynamic systems." *AIAA journal*, 3(8), 1445–1450

[9] Ryall, M. (2007). *Bridge management*. CRC Press.

[10] Simon, D. and Simon, D. L. (2010). "Constrained kalman filtering via density function truncation for turbofan engine health estimation." *International Journal of Systems Science*, 41(2), 159–171

[11] Soetjipto, J. W., Adi, T. J. W., and Anwar, N. (2017). *Bridge Deterioration Prediction Model Based On Hybrid Markov-System Dynamic*, Vol. 138. EDP Sciences.